PCCP

Accepted Manuscript

ROYAL SOCIETY
OF CHEMISTRY

www.rsc.org/pccp

Journal Name

ARTICLE

Impact of Chirality on the Photoinduced Charge Transfer in Linked Systems Containing Naproxen Enantiomers.

E. A. Khramtsova[a,b,†], D. V. Sosnovsky[a,b], A. A. Ageeva[a,b], E. Nuin[c], M. L. Marin[c], P. A. Purtov[a,b], S. S. Borisevich[d], S. L. Khursan[d], H. D. Roth[e], M. A. Miranda[c], V. F. Plyusnin[a,b], T. V. Leshina[a]

The model reaction, the photo-induced donor-acceptor interaction in linked systems - dyads, have been used to study the comparative reactivity of a well-known anti-inflammatory drug, (S)-naproxen (NPX) and its (R)-isomer. (R)- or (S)-NPX in these dyads are linked to (S)-N-methylpyrrolidine (Pyr) using a linear or cyclic amino acid bridge (AA or CyAA), to give (R)-/(S)-NPX-AA-(S)-Pyr flexible and (R)-/(S)-NPX-CyAA-(S)-Pyr rigid dyad. The donor-acceptor interaction is reminiscent of the binding (partial charge transfer, CT) and electron transfer (ET) processes involved in the extensively studied inhibition of the cyclooxygenase enzymes (COXs) by the NPX enantiomers. Besides that, both optical isomers undergo oxidative metabolism by enzymes from P450 family, which also includes ET. The scheme proposed for the excitation quenching of (R)- and (S)-NPX excited state in these dyads is based on the joint analysis of the chemically induced dynamic nuclear polarization (CIDNP) and fluorescence data. The ^{1}H CIDNP effects in this system appear in the back electron transfer in the biradical-zwitterion (BZ), which is formed via dyad's photoirradiation. The rate constants of individual steps in proposed scheme and the fluorescence quantum yields of the local excited states (LE) and exciplexes show stereoselectivity. It depends on the bridge's length, structure and solvent polarity. The CIDNP effects (experimental and calculated) also demonstrate stereodifferentiation. The exciplex quantum yields and the rates of its formation are larger for the dyads containing (R)-NPX that let us suggest the greater contribution from CT processes with (R)-optical isomer.

Introduction

Difference in activity of drugs chiral isomers is currently in scientific focus.[1-4] A good example is the class of non-steroidal anti-inflammatory drugs (NSAIDs), since, despite of a great variety of the chemical structures of NSAIDs, many of them demonstrate different therapeutic activity exactly between optical isomers.[5]

NSAIDs basic activity is the inhibition of the cyclooxygenase enzymes (COXs)[6] which perform the oxygenation of arachidonic acid – precursor of several prostaglandins, potentiating an activity of inflammatory mediators. In recent years NSAIDs analgesic[7] and anti-cancer[8] activity also has drawn attention. At that, their analgesic effect is associated with the inhibition of

endocannabinoids (natural analgesic agents) oxidation by COX 2.[7] And at last, it has been recently observed that the CoA esters of NSAIDs are the substrates of another enzyme – α-metylacyl CoA racemase (AMACR).[8] AMACR levels and activity are associated with some types of cancer (prostate, colon and others).[9] Today the chiral inversion of optically active NSAIDs by AMACR is considered as novel mechanism of their anticancer activity: it is believed that the enzymatically activated conversion of NSAIDs blocks the other harmful effects of a whole group of enzymes – transferases.[8, 10-15] It is worth emphasizing that this activity of NSAID also shows high stereoselectivity.[11,12,14]

In biological chemistry the stereoselectivity of NSAIDs is being investigated, specifically, its main function, the inhibition of COX 2.[16] The COX 2 enzyme has several active sites: the one catalytic site executes a cyclization, another one an oxidation (including an electron transfer (ET)).

Of special interest now is one representative of NSAIDs – naproxen (NPX, 6-methoxy-α-methyl-2-naphthaleneacetic acid) because only the (S)-isomer has anti-inflammatory activity,[17] and it is actually sold as an enantiopure drug. Only (S)-isomer inhibits prostaglandin's synthesis, however, both (R)- and (S)-optical isomers prevent the oxygenation of cannabinoids by COX 2.[7] Whereas (R)-NPX is more active in the processes of metabolic inversion, in particular, by cytochrome P450[18] (which also involves

---
[a.] Institute of Chemical Kinetics and Combustion SB RAS, Institutskaya st., 3, 630090 Novosibirsk, Russia.
[b.] Novosibirsk State University, Pirogova st., 2, 630090 Novosibirsk, Russia.
[c.] Departamento de Química/Instituto de Tecnología Química UPV-CSIC, Universitat Politècnica de València, Camino de Vera s/n, 46022 Valencia, Spain.
[d.] Ufa Institute of Chemistry RAS, Prospect Octyabrya st, 71, 450054 Ufa, Russia
[e.] Rutgers State University, Dept Chem & Chem Biol, Piscataway, NJ 08854 USA.
† Corresponding Author, e-mail: khramtsovaea@gmail.com

ET).[8] At that, according to the results of biochemical research, there is no complete understanding - what kind of physico-chemical interactions are responsible for the difference in the action of (S)- and (R)-NPX.[7,16]

Taking into consideration the abovementioned possible involvement of NPX optical isomers in charge transfer processes, it seems promising to use a model one-electron transfer process for studying the chemical nature of the difference between (S)- and (R)-isomers. Furthermore, the comparison of (S)- and (R)-NPX reactivity in the one of the most universal elementary process –electron transfer may be not only of fundamental but also practical interest.

The stereoselectivity of the photoinduced partial (exciplex) and full charge transfer (biradical-zwitterion, BZ) in the linked system: (R,S)- and (S,S)-NPX-N-methylpyrrolidine has been recently reported.[19-24]

Note that since the days of Jabotinsky works, the photochemical generation of a pair of paramagnetic particles has been using for the modeling of biological processes: the elementary steps of enzymatic oxygenation, drugs– transport proteins binding.[25-27] This approach is considered promising, based on several aspects. Firstly, it can be expected that the reactivity of paramagnetic particles, in a first approximation, does not depend significantly on the way of their generation. Secondly, the greater concentration of short-lived intermediates in comparison with an enzymatic process can be achieved by photogeneration. It allows the use of a variety of physical methods.

In this regard, we are planning to study the chirality impact on the photoinduced processes in (R,S)- and (S,S)-NPX-pyrrolidine dyads, where NPX and a donor are connected by two kind of bridges: flexible and rigid. By the variation of the lengths and structure of bridges we suppose to change the spatial donor-acceptor interaction in the dyad's diastereomers. Since this interaction is believed to determine stereodifferentiation.

We have chosen to use the combination of techniques: fluorescence and chemically induced dynamic nuclear polarization (CIDNP) methods; they have been previously used singly in the research of naproxen dyads.[22-24] It should be noted that the method of the CIDNP is considered as one of the most informative to identify short-living paramagnetic particles[28], and using it together with the fluorescence data can let one to make the quantitative analysis of a process.

As a result, it is planned to establish the main factors affecting the donor-acceptor interaction in (R,S)- and (S,S)-NPX containing dyads with different bridges. In particular, this could allow to trace differences in the reactivity of (R)- and (S)-NPX in processes with partial and full charge transfer.

Results and Discussion

Systems under Study

Two pairs of NPX-pyrrolidine dyads, with a flexible (R)-/(S)-NPX--AA-(S)-Pyr **2 (a,b)** or rigid bridge (R)-/(S)-NPX-CyAA-(S)-Pyr **3 (a,b)** between the donor and acceptor units were designed and synthesized (Synthesis details are presented in Supplementary
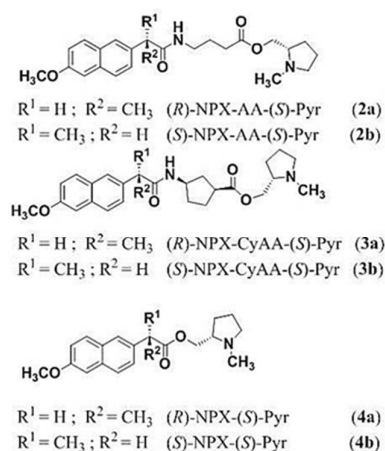

$R^1 = H$; $R^2 = CH_3$	(R)-NPX-ΛΛ-(S)-Pyr (2a)
$R^1 = CH_3$; $R^2 = H$	(S)-NPX-ΛΛ-(S)-Pyr (2b)

$R^1 = H$; $R^2 = CH_3$	(R)-NPX-CyAA-(S)-Pyr (3a)
$R^1 = CH_3$; $R^2 = H$	(S)-NPX-CyAA-(S)-Pyr (3b)

$R^1 = H$; $R^2 = CH_3$	(R)-NPX-(S)-Pyr (4a)
$R^1 = CH_3$; $R^2 = H$	(S)-NPX-(S)-Pyr (4b)

Chart 1 Chemical structure of synthesized dyads.

Information; Chart 1). Thus, (R)- or (S)-NPX **1(a,b)** was reacted with 4-aminobutyric acid or (1S,3R)-3-aminocyclopentanecarboxylic acid to give the corresponding NPX-amino acids that upon esterification using (S)-N-methyl-2-pyrrolidinemethanol resulted in the final dyads (R)-/(S)-NPX-AA-(S)-Pyr **2(a,b)** or (R)-/(S)-NPX-CyAA-(S)-Pyr **3(a,b).** Directly joint (short) (R)-/(S)-NPX-(S)-Pyr dyads **4(a,b)** to be used as controls were prepared as described previously.[20,21]

Fluorescence Quenching of (R,S)- and (S,S)-Dyads

The absorption spectra of both stereoisomers **2 (a,b)** and **3 (a,b)** demonstrate the same bands as the parent NPX **1b**, specifically they display two typical fine-structured UV-absorption bands with maxima at 262 and 332 nm (spectra presented earlier[19-21], for both isomers spectra are equal), which are ascribed to π–π*-type transitions. The fluorescence spectra of **2 (a,b)** and **3 (a,b)** dyads in acetonitrile are presented in Figure 1.

These spectra are similar to the parent NPX but contain an exciplex band in red region. Thus, in addition to a local excited state (LE) an exciplex is also formed under UV irradiation. Its concentration in solution and the position of band's maximum in fluorescence spectra are dependent on permittivity. It is worth noting that the fluorescence quantum yield of **2 (a,b)** LE is higher than that of **3 (a,b)**. Moreover the exciplex band of **2 (a,b)** is much weaker than that of **3 (a,b)**.
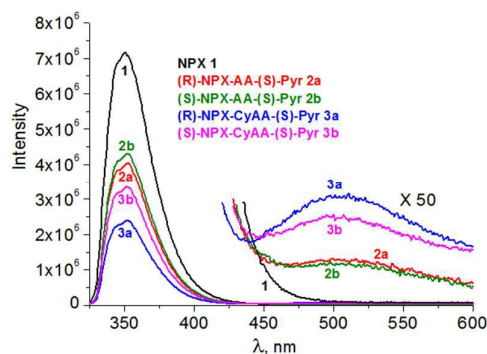

Fig. 1 Fluorescence spectra of **1**, **2 (a,b)** and **3 (a,b)** in acetonitrile (λ_{ex}= 320 nm), concentration ~10^{-5} M. The inset shows magnified emission spectra in the long-wavelength range (> 425 nm).
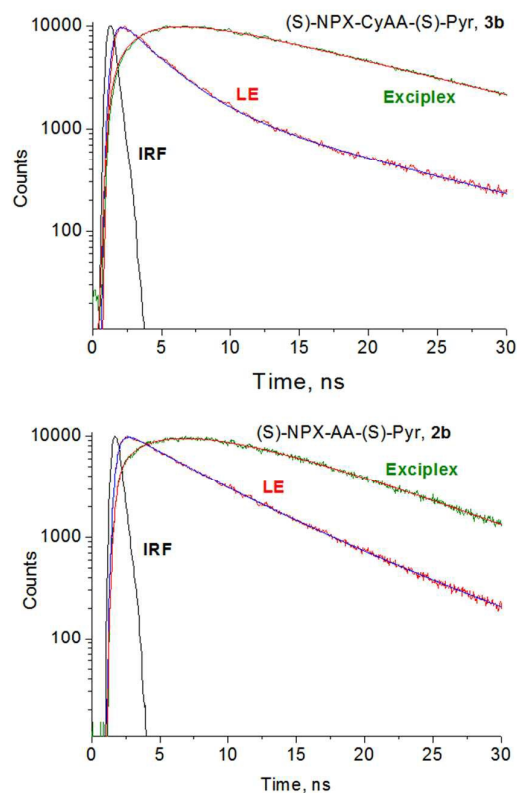
Fig. 2 Fluorescence decay traces of dyad (S)-NPX-AA-(S)-Pyr (**2b**, top) and (S)-NPX-CyAA-(S)-Pyr (**3b**, bottom) at 351 and 500 nm (λ_{ex}= 320 nm) in acetonitrile-benzene mixture (ε = 21.55). IRF − instrument response function.

Typical kinetics curves of LE and exciplex are shown in Figure 2. The two diastereoisomers of **2 (a,b)** and **3 (a,b)** dyads show biexponential kinetics both for LEs and for exciplexes. LE kinetics correspond to two decay times (τ_{short}, τ_{long}), exciplex kinetics - growth and decay times (τ_{rise}, τ_{fall}). The dependence of fluorescence lifetimes on solvent polarity is shown in Figure 3 for **2 (a,b)** and **3 (a,b)**. These curves have been obtained from the experimental data of fluorescence kinetics for dyads in acetonitrile-benzene mixtures (at that $\varepsilon_{acetonirile}$ = 36.8[29], $\varepsilon_{benzene}$ = 2.28[30] and permittivity for mixtures has been taken from the literature[31]). Figure 3 shows, on the one hand, certain correspondence between the values of exciplex decay time (τ_{fall}) and LE long decay time (τ_{long}) and, on the other hand, between exciplex growth time (τ_{rise}) and LE short decay time (τ_{short}). This accordance clearly shows the feedback between the processes of the formation and decay of exciplex and local excited state. Thus, this consideration underlies of the Scheme 1.

This scheme summarizes all the processes taking place in the quenching of the dyads chromophore excitation in the presence of an electron donor. Here, k_1 and k_2 represent pathways through which different dyad conformations (expanded and folded) transfer into the excited states. The first path (k_1) is the formation of LE from an expanded conformation, whereas exciplex, on its turn, is generated from a folded conformation (k_2). So, in rate constants calculations k_1 and k_2 reflect the amount of different conformations participating in the reaction (about 0.8 and 0.2, correspondingly).
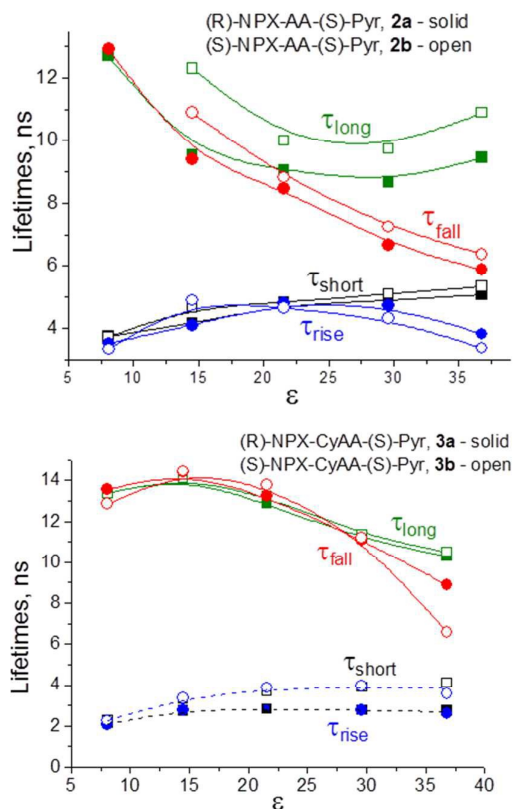

Fig. 3 Dependence on solvent polarity of the fluorescence lifetimes for (R)-/(S)-NPX-AA-(S)-Pyr (**2 (a,b)**, top) and (R)-/(S)-NPX-CyAA-(S)-Pyr (**3 (a,b)**, bottom): local excited state - squares (τ_{short} , τ_{long}) and exciplex - circles (τ_{rise}, τ_{fall}). Lifetimes values are given in the Supplementary Information.

Note that Scheme 1 differs from the scheme proposed earlier for the short **4 (a,b)** dyad.[23,24] In that scheme exciplex is formed only from the local excited state but in our case, for **2 (a,b)** and **3 (a,b)**, the leading edge of exciplex's kinetic curves is satisfactorily fitted only if we assume the simultaneous formation of both exciplex and local excited state. This forced us to assume the existence at least
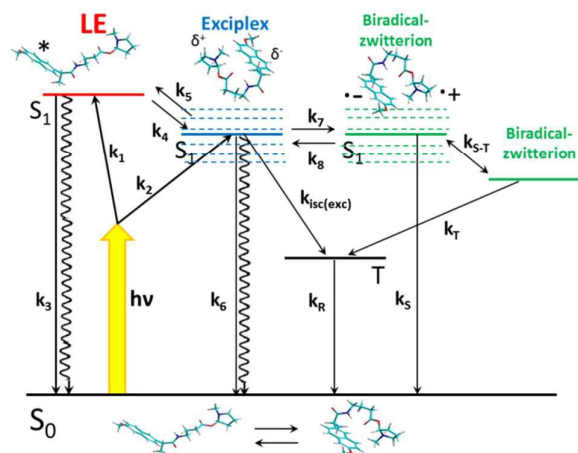
Scheme 1. Quenching mechanism of NPX chromophore in dyads NPX-AA-Pyr **2 (a,b)** and NPX-CyAA-Pyr **3 (a,b)**.

two geometrical conformations of dyads molecules with quite different energies.[32-34]

Exciplex is in rapid dynamic equilibrium with the local excited state (k_4, k_5) and with biradical-zwitterion (k_7, k_8). LE and exciplex emission is presented as k_3 and k_6 constants, correspondingly. BZ can be in singlet or triplet isoenergetic spin states. Spin conversion (k_{S-T}) is taking place under the influence of magnetic interactions in the paramagnetic centers of BZ. Back ET from the both spin states of BZ lead to the formation of the parent dyads in singlet ground and excited triplet state with rate constants k_S and k_T. Both pathways lead to CIDNP of dyads in the ground state. They can be separated since triplet contribution appears delayed by the triplet state lifetime (k_R). Exciplex, in its turn, is also exposed internal conversion with constant $k_{isc(exc)}$. Dotted lines are intended to reflect the dependence of the exciplex and BZ energy levels positions on the dielectric constant of the medium (this relationship is shown in Figure 6 and discussed in detail in the next part).

BZ has been included in the scheme by the analogy with NPX-Pyr **4 (a,b)** dyad, studied previously.[23,24] The conclusion about the equilibrium between exciplex and BZ has been made on the basis CIDNP analysis. Kinetic curves for **2 (a,b)** and **3 (a,b)** dyads have been analyzed by the numerical solution of the system of differential equations by using Runge-Kutta method in the frame of Scheme 1.[35] When solving the differential equations system for all processes in the systems under study, the adequacy of obtained values could be checked only by comparison with available kinetic curves (given that we cannot observe the biradical-zwitterion in these experiments).

It is worth emphasizing that previously studied dyad **4 (a,b)** can also be described by this sequence of steps, outlined in Scheme 1.

Rate constants, related to the processes of the dyad quenching (Scheme 1), are shown in Table 1 for **2 (a,b)** and **3 (a,b)** dyads. The analysis of the data from Table 1 allows us to trace the differences between the diastereomers of studied dyads and compare the results with that for dyads **4 (a,b).** So, the greatest difference is obtained for the rate constants related to the charge transfer: k_4, k_7. At that, the latter shows effect only in polar media. The constant k_4 is greater for the **a)**-isomers of all three dyads (see Figure 4),
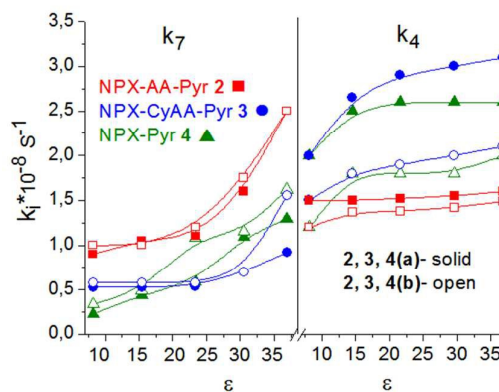

Fig. 4 Correlation between rate constants k_4 (LE to exciplex transition), k_7 (Exciplex to BZ transition) and solvent polarity (see Scheme 1 and Table 1) for **2 (a,b)**, **3(a,b)** and **4(a,b).**

whereas in the case of k_5 no systematic dependence is observed. The rate constant k_7, corresponding to the process of the exciplex transformation into BZ, shows more pronounced dependence on solvent polarity than on an optical configuration (Figure 4).

The dependence of the fluorescence quantum yields of the local excited state (Φ_{LE}) and exciplex (Φ_{exc}) on solvent polarity for both **a)**- and **b)**-diastereomers is shown in Figure 5 (see next page). The analysis of these curves let us conclude that **a)**- diasteromers of dyads comprising (R)-NPX and (S)-N-methylpyrrolidine more inclined to charge transfer (CT) because the rate constants of exciplex formation and its quantum yields are larger than that for **b)**- isomers. As for (S)- NPX, the joint analysis of the exciplex fluorescence quantum yield as well as the corresponding rate constant indicates that in this case exciplex should slightly slower form and quickly decompose. The latter is reflected in its lower Φ_{exc} and larger Φ_{LE} of the dyads consisting (S)-NPX. The comparison of fluorescence quantum yields for all three dyads demonstrates that the stereodifferentiation degree depends on both the bridge's length and its structure. In that way, Φ_{exc} for **a)**- and **b)**-diastereomers differ the most for the short dyad **4**, and much less for **2** dyad with flexible bridge. Meanwhile, the rigid dyad **3** shows

Table 1. Calculated rate constants ($k_i \cdot 10^{-8}s^{-1}$) for pathways outlined in Scheme 1 at different permittivity for NPX-AA-Pyr **2 (a,b)** and NPX-CyAA-Pyr **3 (a,b)** dyads.

| (R)-NPX-AA-(S)-Pyr, 2a						(R)-NPX-CyAA-(S)-Pyr, 3a					
ε	k_3	k_4	k_5	k_6	k_7	ε	k_3	k_4	k_5	k_6	k_7
8.08	0.15	1.5	0.68	0.4	0.9	**8.08**	0.13	2	0.93	0.67	0.53
14.5	0.15	1.5	0.1	0.4	1.05	**14.5**	0.13	2.65	0.45	0.3	0.53
21.55	0.15	1.52	0.07	0.4	1.1	**21.55**	0.13	2.9	0.29	0.3	0.54
29.6	0.15	1.55	0.03	0.4	1.6	**29.6**	0.13	3	0.15	0.3	0.7
36.8	0.15	1.6	0.03	0.4	2.5	**36.8**	0.13	3.1	0.12	0.3	0.92
(S)-NPX-AA-(S)-Pyr, 2b						(S)-NPX-CyAA-(S)-Pyr, 3b					
ε	k_3	k_4	k_5	k_6	k_7	ε	k_3	k_4	k_5	k_6	k_7
8.08	0.15	1.2	0.42	0.63	1.0	**8.08**	0.13	1.5	0.9	0.95	0.58
14.5	0.15	1.37	0.25	0.4	1.0	**14.5**	0.13	1.8	0.4	0.3	0.58
21.55	0.15	1.38	0.1	0.4	1.2	**21.55**	0.13	1.9	0.22	0.3	0.58
29.6	0.15	1.42	0.03	0.4	1.75	**29.6**	0.13	2	0.17	0.3	0.7
36.8	0.15	1.49	0.03	0.4	2.5	**36.8**	0.13	2.1	0.15	0.3	1.55
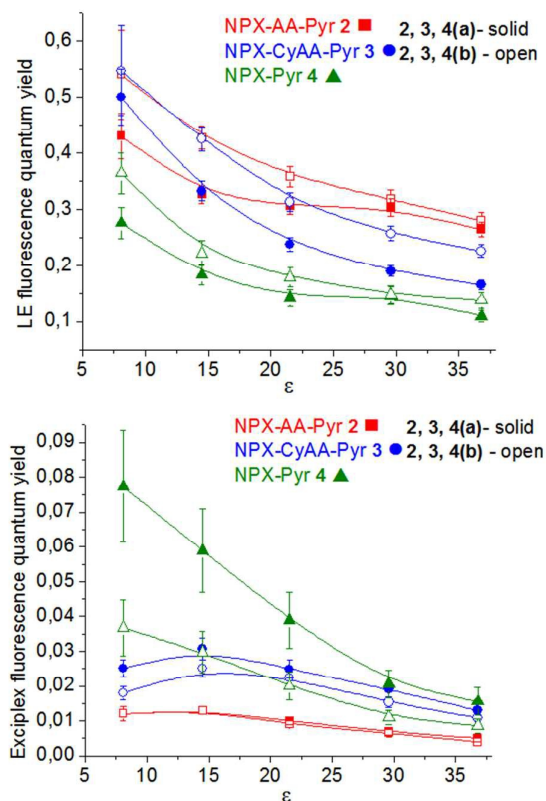
Fig. 5 Fluorescence quantum yield (local excited state, LE – top, exciplex – bottom) dependence on solvent polarity for **2 (a,b)**, **3 (a,b)** and **4 (a,b).** These values have been estimated using NPX in acetonitrile as a standard ($\Phi_{NPX} = 0.47$[21]), numerical values are given in Supplementary Information.

Fig. 6 Dependence of the free energies of the radical-ion pair (RIP) of N-methylpyrrolidine[22]: radical–cation and methoxynaphtalene radical–anion; and exciplex in this system, calculated by using Rehm-Weller equation,[36] top. The dependence of CIDNP effectivity on solvent permittivity for (S)-NPX-AA-(S)-Pyr **2b**, (S)-NPX-CyAA-(S)-Pyr **3b** and (S)-NPX-(S)-Pyr **4b**, bottom.

the stereodifferentiation of Φ_{exc} and Φ_{LE}. The difference in values for **a)**-and **b)**- isomers depends on permittivity less than in other cases. It can be supposed that the contribution of CT states in the quenching process is defined more by the mutual donor- acceptor location than by environment effects.

CIDNP Effects in (R,S)- and (S,S)-Dyads and Their Relationship with "Exciplex - Biradical-Zwitterion" Balance

The high sensitivity of the spin effects in the processes with partially and full CT to polar environments is well-known.[34,37-40] This impact of polarity on CIDNP efficiency has been shown earlier for the photoinduced ET in the short dyad NPX-Pyr **4 (a,b)**.[22,24] Dyads NPX-AA-Pyr **2 (a,b)** and NPX-CyAA-Pyr **3 (a,b)** also demonstrate the dependence of [1]H-CIDNP effects at N- methylpyrrolidine fragments, obtained with a help of pseudo steady state pulses sequence,[41] on the solvent permittivity (see Figure 6, only **b)**-diastereomers are shown). For these dyads the appearance of negative integral polarization of the protons of the N -methyl pyrrolidine fragments of dyads **2 (a,b)** and **3 (a,b)** according to Kaptein rule,[28] corresponds to the back electron transfer in the singlet spin state of BZ. BZ, which, in turn, is obtained from the dyad's singlet excited state.

The position of the dependence extremum (Figure 6) indicates that in dyads with long bridges **2 (a,b)** and **3 (a,b)** maximal CIDNP is
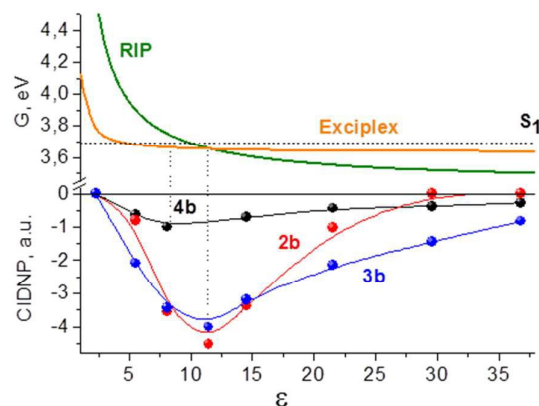
generated at higher polarities where the extremum corresponds to the intersection point of the exciplex and BZ terms. Thus, for **4 (a,b)** dyad the equilibrium is shifted toward the exciplex, whereas for **2 (a,b)** and **3 (a,b)** dyads it is shifted in the direction of the BZ. Indeed, for both **2 (a,b)** and **3 (a,b)** dyads the exciplex quantum yields are significantly lower than those for **4 (a,b)** dyads (see Figure 5). This observation supports the abovementioned concept that the exciplex is formed in the area of the closest approach of donor and acceptor.[34] In essence, there is a certain correlation between the donor-acceptor distance and the "biradical-zwitterion-exciplex" balance. To confirm this hypothesis, as well as to probe the difference between CIDNP polarity dependence for **a)**- and **b)**-diastereomers, the CIDNP effects calculations in the media with different permittivity have been performed. It has been made in the framework of radical pair theory[28] according to the Scheme 1, using the rate constants from Table 1. Other parameters used for the calculation are given in the Supplementary Information.

The curves in Figure 7 (see next page) show satisfactory agreement between theory and experiment. The greatest discrepancies are observed at high polarities. There are several reasons for this: first, the theory has been developed for the motion of the paramagnetic centers of the dyads in the Coulomb field, but it is known that in highly polar media charged particles act as neutrals.[28] The second reason is a change in the relationship of the recombination rates from singlet and triplet BZ's spin states: k_S and k_T, which values are a function of polarity.[22] These changes are not considered in our calculations.

Thus, the simultaneous analysis of CIDNP and fluorescence data allows us to trace all short-lived intermediates involved in the excitation quenching of **2 (a,b)** and **3 (a,b)** dyads; LE, exciplex, and BZ. All of them in any manner depend on the solvent polarity. However, only in the case of CIDNP the source of its dependence is completely understood: it can be explained by a shift of the "exciplex-biradical-zwitterion" equilibrium towards the latter with increasing polarity.
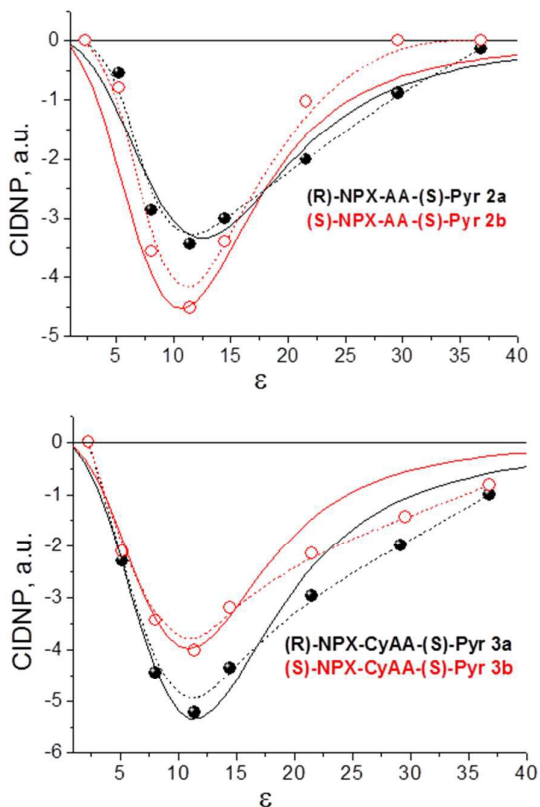
Fig. 7 Dependence of CIDNP effects on solvent polarity for **2(a,b)**, top and **3(a,b)**, bottom. The solid lines are calculated by using the solution of spin chemistry master equation.[28,42,43]

It is interesting to look how the fluorescence quantum yields of exciplex (Φ_{exc}) and local excited state (Φ_{LE}) are related to CIDNP efficiency at different polarities. The analysis of these relations can help to identify the main factors that affect the quantum yields Φ_{exc} and Φ_{LE}. The relationship between CIDNP efficiency for the diastereoisomers of both dyads and the fluorescence quantum yields Φ_{exc} in the media of different permittivity is shown in Figure 8.

As can be seen from Figure 8, the dependence is almost linear, especially for the **a)**-diastereomers. This fully confirms the previously mentioned conclusion, that increasing solvent's permittivity shifts the equilibrium towards BZ. By the way, this correlation allows us to specify the difference between the
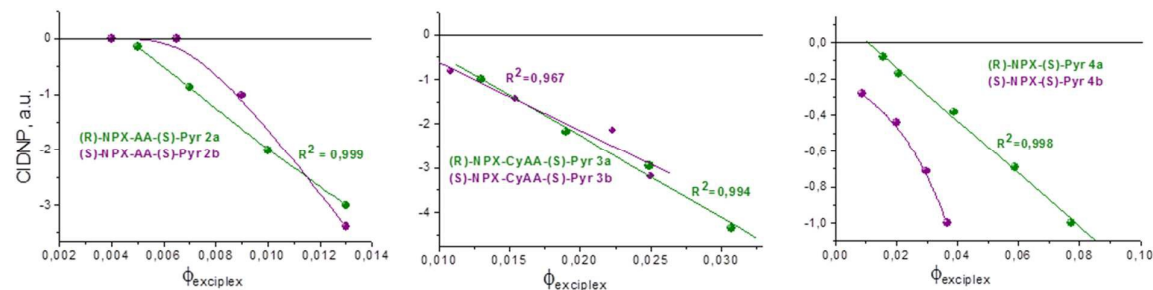
properties of **a)**- and **b)**-diastereomers exciplexes. Because the Φ_{exc} for **a)**-isomers depend on CIDNP effectivity almost linearly, it means that the states with charge transfer contribute majorly in the processes of exciplex's formation and decay. Obviously, that the Φ_{exc} of **b)**-diastereomers, which do not show a linear relationship, depend not only on processes 4 and 7 but also on the 5.

On the other hand, the analysis of the biexponential kinetics of the LE's fluorescence quenching demonstrates that exciplex contributes in this process as well: one exciplex decay channels is its back transformation into LE (Scheme 1). The relationship of Φ_{LE} with CIDNP (not shown), which is not linear, indicates that besides the exciplex back transformation into LE there are other processes which are less sensitive to change in polarity.

To summarize the results of this section we can conclude that the additional confirmation of the reaction Scheme 1 by independent method (with help of the CIDNP analysis) has been obtained. The CIDNP calculation also confirms the existence of the difference between the CIDNP effects of **a)**- and **b)**- diastereomers in the solvents with different permittivity.

Theoretical DFT Conformational Analysis of (R,S)- and (S,S)-Dyads.

Because chiral isomers differ in the mutual arrangement of the substituents at a chiral center, one can expect that the quantum - chemical (QC) conformational analysis of enantiomers and diastereomers help to understand the source of differences in their properties. The majority of works performed in this area is devoted to the conformational analysis of epimers, as well as computational modeling and materials design based on molecular chirality.[44-47]

QC calculations in this work were performed using GAUSSIAN-09 Revision C.1.[48] The most popular DFT method (B3LYP[49,50]) with basis set 6-31G(d)[51] was used for the potential energy surface (PES) scanning and following geometry optimization of the stable conformers found during PES scanning. The structures determined as global minima of the conformational PES were re-optimized using extended basis set 6-311G(d,p).[52] Calculations of vibrational frequencies, enthalpies and Gibbs free energies were performed in the same approximation. Thermodynamic parameters were calculated for the standard conditions (gas phase, 298.15 K and 1 atm) both in the gas phase and in the acetonitrile-benzene binary solvent, the solvent effect was described using the IEFPCM polarized continuum model of Tomasi.[53] Careful conformational analysis was carried out in dyads **4a** and **4b** (Chart 1). Conformational PES was scanned sequentially on five rotation
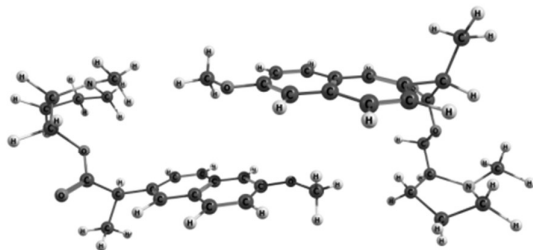

Fig. 8 Correlation between CIDNP effects and the exciplex's fluorescence quantum yields for **2 (a,b)**, left; **3 (a,b)**, middle and **4(a,b)** right.

Fig. 9. The structure of epimers **4a** (left) and **4b** (right) corresponded to the global minima on the conformational PES of molecules (B3LYP/6 311G (d, p) optimization).

axes of the corresponding single bonds between the cyclic moieties of the compounds (technical details are given in the Supplementary Information). As a result, the set of stable compounds were obtained. It was found that the global minima (**4a** and **4b**) on the PES correspond to nearly similar spatial structures, which differ only in the asymmetric C atom of NPX (Figure 9). Maxwell-Boltzmann distribution of the stable conformers was estimated from the Gibbs free energy. For the set of stable conformers the Maxwell-Boltzmann distribution was estimated from the Gibbs free energies. It was revealed that the populations of the most stable conformations for both epimers are similar (28% and 26% for **4a** and **4b** respectively). It may conclude from our theoretical estimations that chirality of the structures do not impact significantly on the energy state distribution of conformers.

Conformational analysis of **4a** and **4b** around 1, 2 and 5 axes allows us to localize stable conformers of dyads with flexible (**2a**, **2b**) and rigid bridge (**3a**, **3b**) at the B3LYP/6-311G(d,p) level of theory. As it was mentioned above for **4a** and **4b**, the equilibrium structures of epimers are similar and differ only in the asymmetric center of naproxen. The thermodynamic parameters (enthalpy and and Gibbs free energies) of epimers were calculated, the relative values of thermodynamic potentials a relatively energy of 2-4a,b were shown in the Table 2. The difference in the values of $H°$ and $G°$ for each epimer pairs does not exceed 2 kJ/mol and, apparently, lies within the error of theoretical estimation.

Based on these results, we can conclude that there is no significant difference in the energy parameters of the dyads, which could reliably explain the experimentally observed differences in photoinduced processes in diastereomers **2-4 (a,b)**.

Table 2. Enthalpies ($\Delta H°$) and Gibbs free energies ($\Delta G°$) of dyads **2-4** relatively to R,S-epimer **(a)** (kJ/mol).

ID structure	Without solvent		MeCN : PhH (60 : 40 V : V)	
	$\Delta H°$	$\Delta G°$	$\Delta H°$	$\Delta G°$
2a	+0.4	+1.5	+0.3	+1.5
2b				
3a	-1.7	-0.4	-0.1	-0.4
3b				
4a	-0.2	-0.4	-0.4	-0.9
4b				

Conclusions

Remarks Concerning Features of the Behaviour of Dyads with (S)- and (R)-Naproxen

It is interesting to compare the peculiar properties of the (*R*,*S*)- and (*S*,*S*)- NPX-AA-Pyr, NPX-CyAA-Pyr, NPX-Pyr dyad's reactivity in the model charge transfer (CT) processes with the difference between some activity of (R)- and (S)-NPX in biological systems. Namely, only (S)-NPX is a real inhibitor of arachidonic acid oxygenation[16] (anti-imflammatory effect) but all (R)-isomers of 2 - aryl propionyl derivatives are potent inhibitors of endocannabinoid oxygenation[7] (analgetic effect) and (R)-NPX more actively undergoes to chiral metabolism.[8] Our results show the prevailing of (R,S)-dyad's exciplex fluorescence quantum yields (Φ_{exc}, up to two times) and the rate constants of the exciplex formation (k_4, in half times), as well as the different CIDNP effects of optical isomers.

The difference between Φ_{exc} and k_4 let us suggest that the contribution of CT processes is larger for dyads comprising (R)-NPX. This suggestion is also confirmed by the linear relation between the Φ_{exc} of (R,S)-dyads isomers and the CIDNP efficiency, which is completely determined by the equilibrium "exciplex–biradical-zwitterion."

According to these results, it can be assumed that **(**R)-NPX should be more active in the processes of the chiral metabolism by the action of cytochrome P450, which involves electron transfer.[18] Indeed, in the oxidative metabolism of (R)-/(S)-NPX by the microsomal fraction of P450, v_{max}/K_m ratio is bigger in 1.3 times for the (R)-isomer.[54] However, in the case of the chiral inversion of NPX-CoA esters by non P450 pathways (AMACR and other transferases) (R)-isomer demonstrates many times greater activity than the (S)-.[8,12,13,55]

Saying about **(**S)-NPX, it is known that it acts as a weak reversible inhibitor of COX 2.[7] Since we believe that our model charge transfer reaction might be reminiscent of the donor-acceptor binding, the smaller Φ_{exc} of **(**S,S)-dyads and their larger Φ_{LE} are correspond to the idea about larger (S)-NPX binding reversibility. Note that this conclusion is in an agreement with the results of biochemical research.[7]

Altogether, obtained results have demonstrated that the stereodifferentiation of diastereomeric (R,S)- and (S,S)-dyads depends on the length of the bridge and on its structure. The relative proximity of the donor and the acceptor results in the largest difference in the reactivity of the diastereomers. This indicates that differences in the reactivity of the optical isomers can be sensitive to the relative position of partners, for example, in active sites.

Acknowledgements

## Notes and references

1 G.-Q. Lin, Q.-D. You, J. F. Cheng, Chiral Drugs: Chemistry and Biological Action, 1st ed; John Wiley & Sons Inc., New Jersey, USA, 2011.

2 K. Krasulova, M. Siller, O. Holas, Z. Dvorak, P. Anzenbacher, *Xenobiotica*, 2015, 1-10.

3 Q. Shen, L. Wang, H. Zhou, H. Jiang, L. Yu, S. Zeng, *Acta Pharm. Sinic.*, 2013, **34**, 998-1006.

4 C.-R. Chong, N. E. Drury, G. Iicari, M. P. Frenneaux, J. D. Horowitz, D. Pagano, B. C. Sallustio, *Eur. J. Clin. Pharmacol.*, 2015, 1-7.

5 A. M. Evans, *Eur. J. Clin. Pharmacol.*, 1992, **42**, 237-256.

6 R. J. Flower, *J. Pharmacol. Rev.*, 1974, **26**, 33-67.

7 K. C. Duggan, D. J. Hermanson, J. Musee, J. J. Prusakiewicz, J. L. Scheib, B. D. Carter, S. Banerjee, J. A. Oates, L. J. Marnett, *Nature Chem. Biol.*, 2011, **7**, 803-809.

8 T. J. Woodman, P. J. Wood, A. S. Thompson, T. J. Hutchings, G. R. Steel, P. Jiao, M. D. Threadgill, M. D. Lloyd, *Chem. Commun.*, 2011, **47**, 7332-7334.

9 M. D.Lloyd, D. J. Darley, A. S. Wierzbicki, M. D. Threadgill, *FEBS J.*, 2008, **275**, 1089-1102.

10 C.-S. Chen, W.-R. Shieh, P.-H. Lu, S. Harriaman, C.-Y. Chen, *Biochim. Biophys. Acta*, 1991, **1078**, 411-417.

11 R. D. Knihincki, R. O. Day, K. M. Williams, *Biochem. Pharmacol.,* 1991, **42**, 1905-1911.

12 C. Sevoz, E. Benoit, T. Buronfosse, *Drug Metabol. Dispos.*, 2000, **28**, 398-402.

13 M. P. Knadler, S. D. Hall, *Chirality*, 2004, **16**, 379-387.

14 F. Jamali, R. Lovlin, G. Aberg, *Chirality*, 1997, **9**, 29-31.

15 D. D. Leipold, D. Kantoci, E. D. Murray Jr., D. D. Quiggle, W. J. Wechter, *Chirality*, 2004, **16**, 379-387.

16 K. C. Duggan, M. J. Walters, J. Musee, J. M. Harp, J. R. Kiefer, J. A. Oaters, L. J. Marnett, *J. Biol. Chem.*, 2010, **285**, 34950-34959.

17 W. F. Kean, C. J. L. Lock, J. Rischke, R. Butt, W. W. Buchanan, H. Howard-Lock, *J. Pharm. Sci.*, 1989, **78**, 324-327.

18 J. O. Miners, S. Coulter, R. H. Tukey, M. E. Veronese, D. J. Birkett, *J. Biochem. Pharmacol.*, 1996, **51**, 1003-1008.

19 U. Pischel, S. Abad, M. A. Miranda, *Chem. Commun.*, 2003, 1088-1089.

20 S. Abad, U. Pischel, M. A. Miranda, *Photochem. Photobiol. Sci.*, 2005, **4**, 69-74.

21 M. C. Jimenez, U. Pischel, M. A. Miranda, *J. Photochem. Photobiol. C*, 2007, **8**, 128-142.

22 I. M. Magin, N. E. Polyakov, E. A. Khramtsova, A. I. Kruppa, Yu. P. Tsentalovich, T. V. Leshina, M. A. Miranda, E. Nuin, M. L. Marin, *Chem. Phys. Lett.*, 2011, **516**, 51-55.

23 E. A. Khramtsova, V. F. Plyusnin, I. M. Magin, A. I. Kruppa, N. E. Polyakov, T. V. Leshina, E. Nuin, M. L. Marin, M. A. Miranda, *J. Phys. Chem. B*, 2013, **117**, 16206-16211.

24 I. M. Magin, N. E. Polyakov, E. A. Khramtsova, A. I. Kruppa, A. A. Stepanov, P. A. Purtov, T. V. Leshina, Yu. P. Tsentalovich, M. A. Miranda, E. Nuin, et al, *Appl. Magn. Reson.*, 2011, **41**, 205-220.

25 F. I. Ataullahanov, A. M. Jabotinsky, *Biofizika+*, 1975, **20**, 596-601.

26 M. S. Afanasyeva, M. B. Taraban, P. A. Purtov, T. V. Leshina, C. B. Grissom, *J. Am. Chem. Soc.*, 2006, **128**, 8651-8658.

27 N. E. Polyakov, M. B. Taraban, T. V. Leshina, *Photochem. Photobiol.*, 2004, **80**, 565-571.

28 K. M. Salikhov, Yu. N. Molin, R. Z. Sagdeev, A. L. Buchachenko, Spin Polarization and Magnetic Effects in Radical Reactions, Akademiai Kiado, Budapest, Hungary, 1984.

29 G. P. Cunningham, J. A. Vidulich, R. L. Kay, *J. Chem. Eng. Data*, 1967, **12**, 336-337.

30 A. A. Mariott, E. R. Smith, Table of Dielectric Constants of Pure Liquids, NBS: Washington, DC, 1951.

31 Y. J. Ahadov, Dielectricheskie Svoystva Binarnyh Rastvorov, Nauka, Russia, 1977.

32 I. Azumaya, H. Kagechika, Y. Fujiwara, M. Itoh, K. Yamaguchi, K. J. Shudo, *J. Am. Chem. Soc.*, 1991, **113**, 2833-2838.

33 S. Olsen, R. H. McKenzie, *J. Chem. Phys.*, 2012, **137**, 164319.

34 K. Bhattacharyya, M. Chowhurry, *Chem. Rev.*, 1993, **93**, 507-535.

35 J. C. Butcher, Numerical Methods for Ordinary Differential Equations, Wiley, 2003.

36 D. Rehm, A. Weller, *Ber. Bunsen. Phys. Chem.*, 1969, **73**, 834-839.

37 U. Werner, H. Staerk, *J. Phys. Chem.*, 1995, **99**, 248-256.

38 K. Pal, D. R. Kattnig, G. Grampp, S. Landgraf, *Phys. Chem. Chem. Phys.*, 2012, **14**, 3155-3161.

39 S. Bandyopadhyay, K. Sen, S. D. Choudhury, S. Basu, *RIKEN Review*, 2002, **44**, 56-58.

40 S. Richert, A. Rosspeinter, S. Landgraf, G. Grampp, E. Vauthey, D. R. Kattnig, *J. Am. Chem. Soc.*, 2013, **135**, 15144-15152.

41 M. Goez, Pseudo Steady-State Photo-CIDNP measurements. *Chem. Phys. Lett.* 1992, **188**, 451-456.

42 P. A. Purtov, A. B. Doktorov, *Chem. Phys.*, 1993, **178**, 47-65.

43 A. Parnachev, P. Purtov, E. Bagryanskaya, R. Sagdeev, *J. Chem. Phys.*, 1997, **107**, 9942-9953.

44 J. Moreno, F. Urena, J. Gonzalez, *Vib. Spectrosc.*, 2009, **51**, 318-325.

45 H. J. Jensen, J. olsen, Advances in Quantum Chemistry. 1st ed, *Academic Press*, 2005.

46 A. Baev, M. Samoc, P. N. Prasad, M. Krykunov, J. Autschbach, *Opt. Express*, 2007, **15**, 5730-5741.

47 J. Moreno, F. Urena, J. Gonzalez, *Struct. Chem.*, 2011, **22**, 67-76.

48 M. J. Frisch, G. W. Trucks, H. B. Schlegel, G. E. Scuseria, M. A. Robb, J. R. Cheeseman, G. Scalmani, V. Barone, B. Mennucci, G. A. Petersson, H. Nakatsuji, M. Caricato, X. Li, H. P. Hratchian, A. F. Izmaylov, J. Bloino, G. Zheng, J. L. Sonnenberg, M. Hada, M. Ehara, K. Toyota, R. Fukuda, J. Hasegawa, M. Ishida, T. Nakajima, Y. Honda, O. Kitao, H. Nakai, T. Vreven, J. Montgomery, J. A., J. E. Peralta, F. Ogliaro, M. Bearpark, J. J. Heyd, E. Brothers, K. N. Kudin, V. N. Staroverov, R. Kobayashi, J. Normand, K. Raghavachari, A. Rendell, J. C. Burant, S. S. Iyengar, J. Tomasi, M. Cossi, N. Rega, J. M. Millam, M. Klene, J. E. Knox, J. B. Cross, V. Bakken, C. Adamo, J. Jaramillo, R. Gomperts, R. E. Stratmann, O. Yazyev, A. J. Austin, R. Cammi, C. Pomelli, J. W. Ochterski, R. L. Martin, K. Morokuma, V. G. Zakrzewski, G. A. Voth, P. Salvador, J. J. Dannenberg, S. Dapprich, A. D. Daniels, Ö. Farkas, J. B. Foresman, J. V. Ortiz, J. Cioslowski, D. J. Fox, Gaussian 09, Revision C.1, Gaussian, Inc., Wallingford CT, 2009.

49 A. D. Becke, *J. Chem. Phys.*, 1993, **98**, 5648.

50 C. Lee, W. Yang, R. G. Parr, *Phys. Rev. B: Condens. Matter*, 1988, **37**, 785.

51 W. J. Hehre, R. Ditchfield, J. A. Pople, *J. Chem. Phys.*, 1972, **56**, 2257.

52 K. Raghavachari, J. S. Binkley, R. Seeger, J. A. Pople, *J. Chem. Phys.*, 1980, **72**, 650.

53 J. Tomasi, B. Mennucci, R. Cammi, *Chem. Rev.*, 2005, **105**, 2999-3094.

54 S. Sanoh, A. Horigushi, K. Sugihara, Y. Kotake, Y. Tayama, N. Uromaru, H. Ohshita, Ch. Tateno, T. Horie, Sh. Kitamura, Sh. Otha, *Drug Metab. Dispos.*, 2012, **40**, 2267-2272.

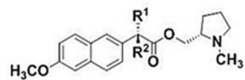55 M. El Mouelhi, H. W. Ruelius, C. Fenselau, D. M. Dulik, *Drug Metab. Dispos.,* 1987, **15**, 767-772.
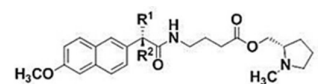
$R^1 = H$; $R^2 = CH_3$ (R)-NPX-AA-(S)-Pyr   (2a)
$R^1 = CH_3$; $R^2 = H$ (S)-NPX-AA-(S)-Pyr   (2b)
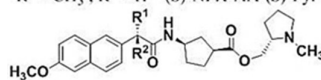
$R^1 = H$; $R^2 = CH_3$ (R)-NPX-CyAA-(S)-Pyr   (3a)
$R^1 = CH_3$; $R^2 = H$ (S)-NPX-CyAA-(S)-Pyr   (3b)

$R^1 = H$; $R^2 = CH_3$ (R)-NPX-(S)-Pyr   (4a)
$R^1 = CH_3$; $R^2 = H$ (S)-NPX-(S)-Pyr   (4b)

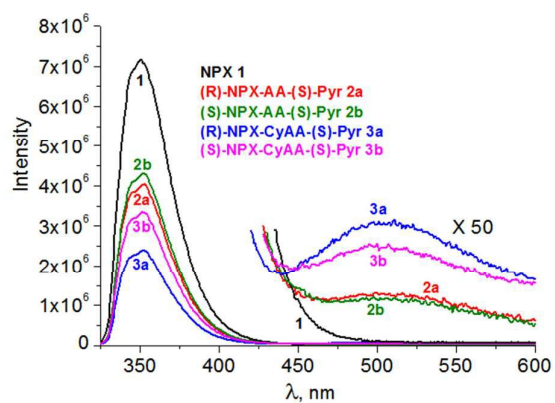**Chart 1** Chemical structure of synthesized dyads.

Fig. 1 Fluorescence spectra of **1**, **2 (a,b)** and **3 (a,b)** in acetonitrile (λ_{ex}= 320 nm), concentration ~10^{-5} M. The inset shows magnified emission spectra in the long-wavelength range (> 425 nm).
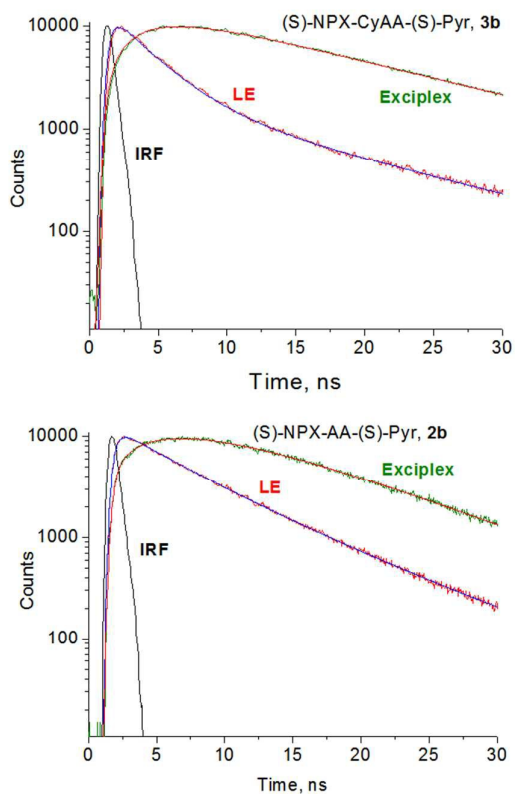
Fig. 2 Fluorescence decay traces of dyad (S)-NPX-AA-(S)-Pyr (**2b**, top) and (S)-NPX-CyAA-(S)-Pyr (**3b**, bottom) at 351 and 500 nm (λ_{ex}= 320 nm) in acetonitrile-benzene mixture (ε = 21.55). IRF – instrument response function.
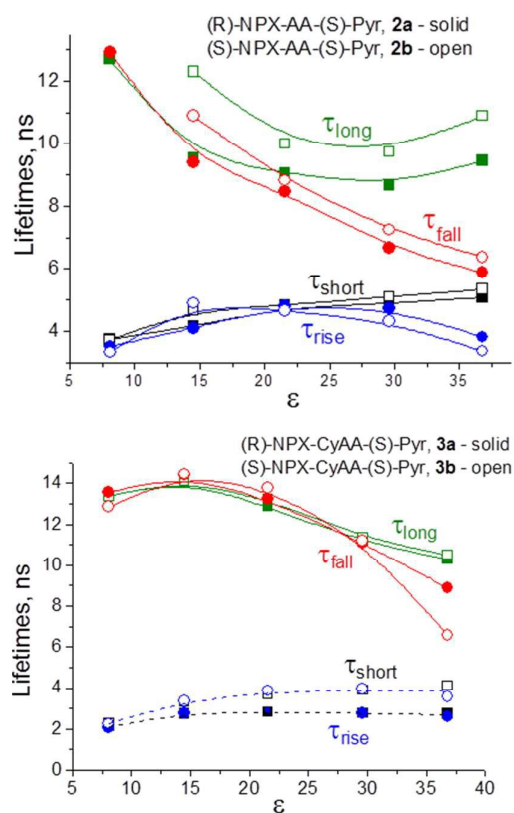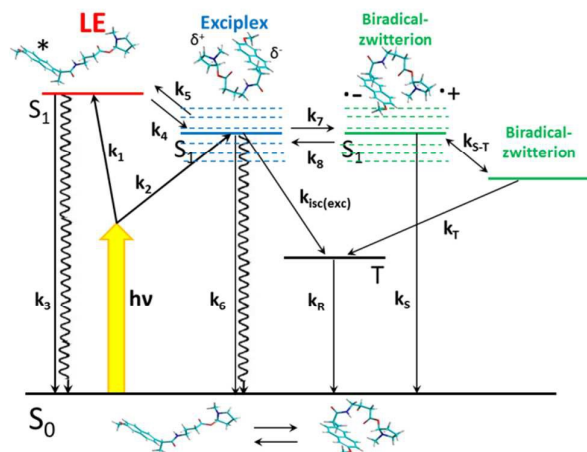
Fig. 3 Dependence on solvent polarity of the fluorescence lifetimes for (R)-/(S)-NPX-AA-(S)-Pyr (**2 (a,b)**, top) and (R)-/(S)-NPX-CyAA-(S)-Pyr (**3 (a,b)**, bottom): local excited state - squares (τ_{short} , τ_{long}) and exciplex - circles (τ_{rise}, τ_{fall}). Lifetimes values are given in the Supplementary Information.

Scheme 1. Quenching mechanism of NPX chromophore in dyads NPX-AA-Pyr **2 (a,b)** and NPX-CyAA-Pyr **3 (a,b)**.

Fig. 4 Correlation between rate constants k_4 (LE to exciplex transition), k_7 (Exciplex to BZ transition) and solvent polarity (see Scheme 1 and Table 1) for **2 (a,b), 3(a,b)** and **4(a,b).**
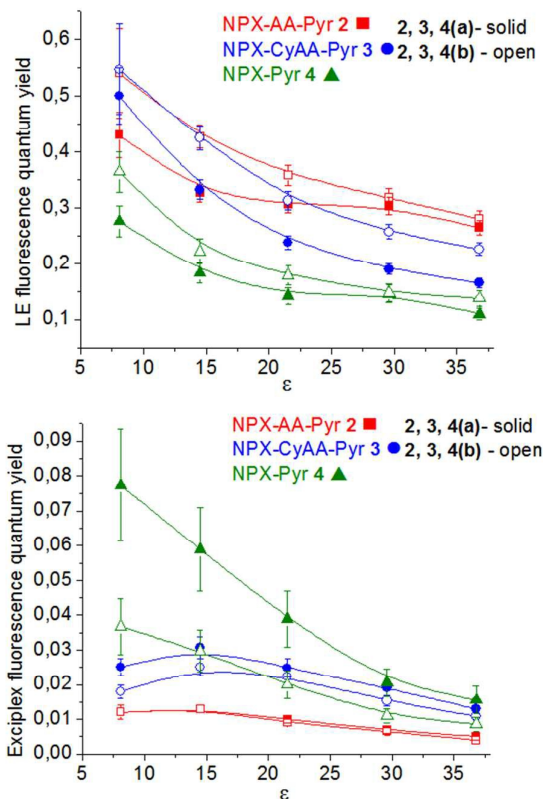
Fig. 5 Fluorescence quantum yield (local excited state, LE – top, exciplex – bottom) dependence on solvent polarity for **2 (a,b)**, **3 (a,b)** and **4 (a,b).** These values have been estimated using NPX in acetonitrile as a standard (Φ_{NPX} = 0.47[21]), numerical values are given in Supplementary Information.
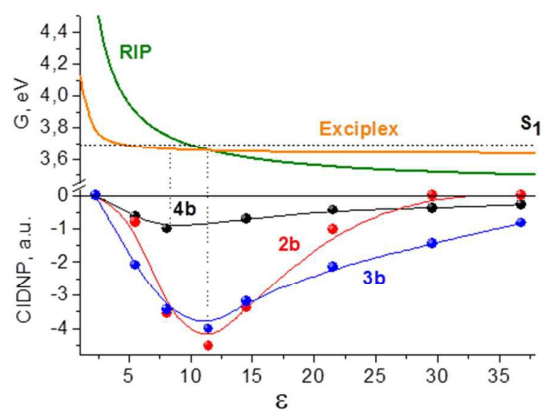
ARTICLE

Journal Name

Fig. 6 Dependence of the free energies of the radical-ion pair (RIP) of N-methylpyrrolidine[22]: radical–cation and methoxynaphtalene radical–anion; and exciplex in this system, calculated by using Rehm-Weller equation,[36] top. The dependence of CIDNP effectivity on solvent permittivity for (S)-NPX-AA-(S)-Pyr **2b**, (S)-NPX-CyAA-(S)-Pyr **3b** and (S)-NPX-(S)-Pyr **4b**, bottom.
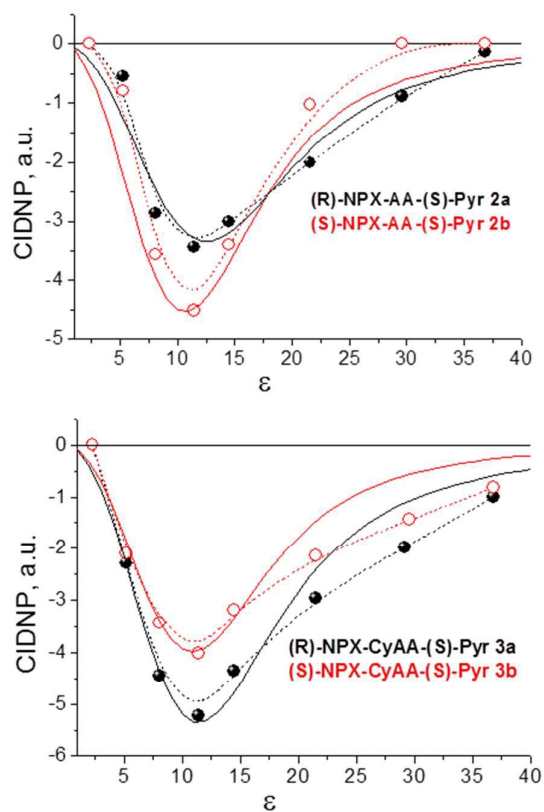
Fig. 7 Dependence of CIDNP effects on solvent polarity for **2(a,b)**, top and **3(a,b)**, bottom. The solid lines are calculated by using the solution of spin chemistry master equation.[28,42,43]
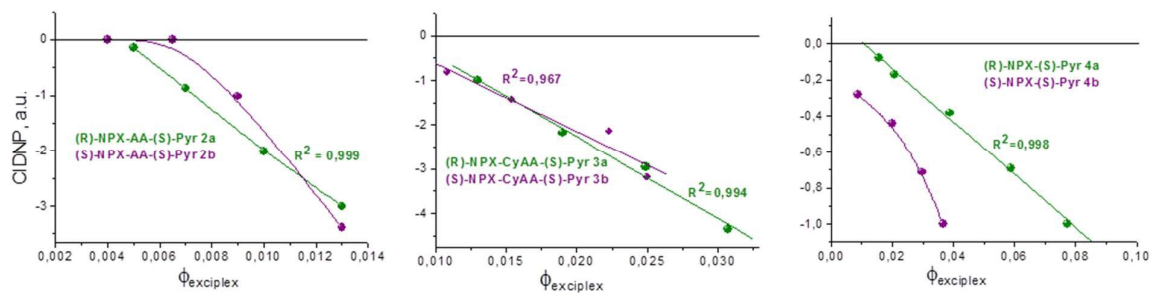
Fig. 8 Correlation between CIDNP effects and the exciplex's fluorescence quantum yields for **2 (a,b)**, left; 3 **(a,b)**, middle and **4(a,b)** right.
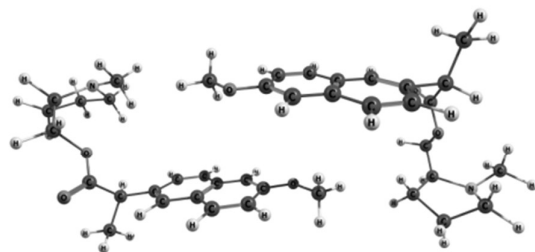
Fig. 9. The structure of epimers **4a** (left) and **4b** (right) corresponded to the global minima on the conformational PES of molecules (B3LYP/6 311G (d, p) optimization).